miRNA Detection on Printed Electrochemical Strips Empowered by Hybridization Chain Reaction

Ada Raucci [1], Assunta Anna Santillo [1], Luca Capelli [2], Antonio Giordano[3,4] Alessandro Bertucci [2*], Stefano Cinti [1,3*]

[1] Department of Pharmacy, University of Naples Federico II, Naples, Italy

[2] Department of Chemistry, Life Sciences and Environmental Sustainability, University of Parma, Parma, Italy

[3] Sbarro Institute for Cancer Research and Molecular Medicine, Center for Biotechnology, College of Science and Technology, Temple University, Philadelphia, PA 19122, USA

[4] Department of Medical Biotechnologies, University of Siena, 53100 Siena, Italy.

Corresponding authors: Alessandro.bertucci@unipr.it; Stefano.cinti@unina.it

Abstract

Printed electrochemical strips are increasingly used in nucleic acid diagnostics due to their affordability portability, compactness, and ease of use. To respond to traditional electrochemical methods that require complex immobilization protocols, in this study, we introduce a simplified platform that combines a cost-effective electrode printed on a polyester substrate with a hybridization chain reaction (HCR) for DNA signal amplification. Unlike prior approaches that rely on nanomaterials or intricate modifications, our method places the target sequence and hairpins directly on the electrode surface, reducing both cost and preparation time while maintaining efficient signal amplification. Using DNA modified with methylene blue (MB) as a redox mediator, the system generates a "signal-off" response by suppressing electron transfer when MB intercalates into the DNA polymers formed by HCR. This approach eliminates the need for complex surface functionalization, enhancing ease of fabrication and consistency. Targeting miRNA-21, a known cancer biomarker, the sensor achieves picomolar sensitivity in both buffer and diluted human serum. This platform offers a cost-effective, sensitive, and portable solution for point-of-care diagnostics and real-time miRNA monitoring in clinical settings.

Introduction

MicroRNAs (miRNAs) are small non-coding RNA molecules that play crucial roles in gene expression and metabolic functions.[1] They have garnered considerable attention for their ability to modulate cellular mechanisms, influencing cell proliferation, angiogenesis, cancer metastasis and drug resistance.[2–5] Among the various miRNAs, miRNA-21 has emerged as one of the most widely studied due to its prominent role in oncogenesis and other pathological conditions.[6] Given their pivotal role in important cellular processes, miRNAs, including miRNA-21, are considered valuable indicators of disease progression and promising targets for treatment strategies[7–10] Therefore, detection and quantification of miRNAs in diseases are essential to understand their role in biological processes and their potential as biomarkers.

Several techniques have been developed for the detection of miRNAs, each with its own advantages and limitations, including Northern blotting,[11] quantitative real-time PCR (qRT-PCR),[12] and microarrays.[13] While these methods offer high sensitivity and specificity, they also involve higher cost and complexity, limitings their widespread application. For example, PCR-based detection requires short primers that reduce efficiency and increase the risk of non-specific amplification. Additionally, the low concentration of miRNA in cells and blood also limits the sensitivity of Northern blotting, making it inadequate for detecting nanomolar or even lower concentrations. Despite their high throughput, microarrays suffer from cross-hybridization and low

sensitivity.[14,15] To address these challenges, innovative techniques such as colorimetric,[16] fluorescent[17] and electrochemical methods are being developed for miRNA detection.[18] Although, many of these techniques utilize cutting-edge technology, they often necessitate multiple reactions or signal transformation steps. Here, we addressed these biosensing challenges by employing electrochemical strips as promising biosensors offering low cost, immediacy, miniaturisation and rapid response.[19–21] However, a challenge in designing electrochemical biosensors is precisely controlling the density and orientation of the recognition probes on the electrode surface, as these parameters are critical for defining their response window and sensitivity.[22–24]

To tackle these challenges and further improve the sensitivity of electrochemical biosensors, several chemical and biological amplification strategies have been proposed. [25–27]Among these, the hybridization chain reaction (HCR) has emerged as a promising technique. HCR is a DNA polymerization cascade triggered by initiator or target molecules, leading to the formation of long DNA chains from short oligonucleotide hairpins.[28,29] This isothermal amplification method leverages the self-assembly of two rationally designed DNA hairpins to produce amplified signals in the presence of a target molecule.[30,31] When a trigger strand initiates the chain reaction, it consecutively opens the hairpin structures, causing them to hybridize in a self-sustained process and form long DNA polymers, significantly enhancing the detection signal and enabling the identification of target molecules at very low concentrations.[32,33] Compared to other amplification techniques, HCR offers superior advantages, such as low background noise, cost-effectiveness, and greater stability, making it a powerful tool for developing sensitive biosensors.[34,35]

Several electrochemical methods for miRNA detection harnessing HCR amplification have been reported.[36–41] However, these methods often require the use of specific nanomaterials or involve labor-intensive and time-consuming electrode modification procedures. To address these limitations, in the present work, we developed an innovative platform for the detection of miRNA-21 that integrates a cost-effective polyester electrode combined with HCR amplification. The use of HCR as signal amplification strategy enhances sensitivity and greatly simplifies the manufacturing process, achieving a detection limit at the picomolar level without the need for electrode surface modification. By eliminating complex surface functionalization procedures, this advancement facilitates fabrication and reduces inconsistencies. In our approach, the sample is applied directly to the electrode surface, significantly lowering both the overall cost and time required for analysis. The DNA hairpins used in the sensor were modified with methylene blue (MB) as a redox mediator. The HCR technique enables signal amplification through a signal-off mechanism, where electron transfer is substantially reduced when the redox mediators become intercalated within the self-assembled DNA polymers, thereby enabling highly sensitive miRNA detection. This proposed platform leverages the principles of the hybridization chain reaction for the sensitive detection of miRNA-21, offers a robust, cost-effective system with great potential for point-of-care (PoC) diagnostics and real-time monitoring of miRNA levels in clinical settings.

Experimental section

Reagents and apparatus

All reagents used were of the highest quality available. PBS tablets (140 mM NaCl, 10 mM phosphate buffer, 3 mM KCl), and human serum were purchased from Sigma-Aldrich (St. Louis, MO, USA). The DNA hairpin probes, specifically hairpin H1 (5'-Atto MB2-ATC AGT CTG ATA AGC TAC TAA CTT AGC TTA TCA G-3') and hairpin H2 (5'-Atto MB2-TAG CTT ATC AGA CTG ATC TGA TAA GCT AAG TTA G-3'), along with the target sequence miRNA-21 (5'-uag cuu auc aga cug aug uug-3'), were obtained from Metabion GmbH (Steinkirchen, Germany). Sequences tested as potential interferents, including miRNA-218 (5'-uug ugc auc uaa cca ugu-3'), miRNA-29c-5p (5'-uga ccg auu ucu ccu ggu guu-3'), and miR652-5p (5'-caa ccc uag gag ggg gug cca uuc-3'), were also sourced from Metabion GmbH (Steinkirchen, Germany). Adobe Illustrator was used to draw the wax model of the creation of the hydrophilic test area on the filter- paper electrodes. A solid ink printer, the ColorQube 8580 from Xerox (USA), was used to print the hydrophobic wax layer.

Fabrication of electrochemical strips

Graphite-based polyester screen-printed electrodes (SPE) with a three-electrode configuration were produced in-house by manual screen printing onto a flexible polyester film substrate, Autostat HT5 (125 µm), MacDermid, UK. The three-electrode design was created manually using a squeegee to distribute the conductive inks through a specially designed mask. Specifically, Ag/AgCl ink (Loctite, Italy) was used to print the connections and reference electrode, while carbon ink (Sun Chemical, USA) was used for the working and contrast electrodes. After printing, the strips were thermally cured at 100 °C for 30 minutes, making the ink stable for electrochemical measurements. The diameter of the working electrode was 0.4 cm, while the electrochemical strips measured approximately 2.5 cm high and 1 cm wide. To prevent the spread of aqueous samples towards the connector, adhesive tape was applied to delimit the test area. Regarding the fabrication of the filter paper electrodes, before printing the silver and graphite layer, we followed the process illustrated below: the final model of the paper device was created using Adobe Illustrator and then printed on Whatman No. 1 chromatographic paper with wax-based ink. After printing, the wax paper was placed in an oven at 100 °C for 1 minute. This procedure allowed the wax to penetrate through the paper, forming a hydrophobic layer around the hydrophilic test area. This hydrophobic layer is crucial for clearly defining the test area and limiting the diffusion of the solution within the electrochemical cell.[42]

Electrochemical Measurements

All electrochemical measurements were performed with a Multi Emstat 4 portable potentiostat (PalmSens, Netherlands) equipped with a multi-8 reader and interfaced with a laptop running PSTrace 5.9 software. All reported potentials refer to the Ag/AgCl reference pseudo-electrode of the screen-printed electrochemical strips. Square wave voltammetry (SWV) was used to analyse the biosensor surfaces with the samples. SWV voltammograms were collected using a frequency of 50 Hz, an equilibrium time of 5 s, an E step of 0.001 V, an amplitude of 0.01 V and a potential window between 0 and -0.5 V, as previously optimised.[43]

HCR-amplified electrochemical miRNA detection

The buffer used for the electrochemical measurements and preparation of the H1, H2 and miRNA-21 solutions was a PBS buffer at pH 7.4, containing 140 mM NaCl, 10 mM phosphate and 3 mM KCl.

Regarding the experimental procedure, DNA hairpin solutions, H1 and H2, both modified with MB as a redox mediator, were mixed together to a desired final concentration and then incubated in an Eppendorf for 30 minutes, both in the absence and in the presence of different concentrations of miRNA-21. After the incubation time had elapsed, a volume of 50 µL was taken and placed directly on the working area of the electrode. The current intensity was measured for samples containing only H1 and H2 compared to those containing different miRNA-21 concentrations. For all measurements, the signal variation (%) was evaluated as: signal variation (%) = $(I_0 - I_{target}) / I_0 \times 100$, where I0 is the signal obtained in the absence of miRNA and I_{target} is the signal obtained in the presence of miRNA. The same procedure was performed for both standard and human serum measurements.

Results and discussion

Evaluation of the experimental setup

Optimisation of the experimental parameters for the electrochemical biosensor was performed in a standard phosphate buffer solution at pH 7.4 to ensure optimal analytical performance in target detection. Measurements were conducted simultaneously on eight electrodes using an eight-channel multiplexer potentiostat.

As previously mentioned, the two DNA hairpins, H1 and H2, were designed to remain in a closed conformation in the absence of miRNA-21, thus maintaining a stable electrochemical signal due to the MB tags conjugated at their 5'-end. In this conformation, the MB tags are freely available for efficient electron transfer with the electrode surface. We hypothesized that when miRNA-21 is present and triggers the hybridization chain

reaction between H1 and H2, the resulting long DNA polymers would cause the MB tags to become intercalated within the polymer structure, pulling them away from the electrode surface. This sequestration effect is expected to drastically reduce the efficiency of the electron transfer process, leading to a decrease in the electrochemical signal and enabling a signal-off mechanism. (Scheme 1).

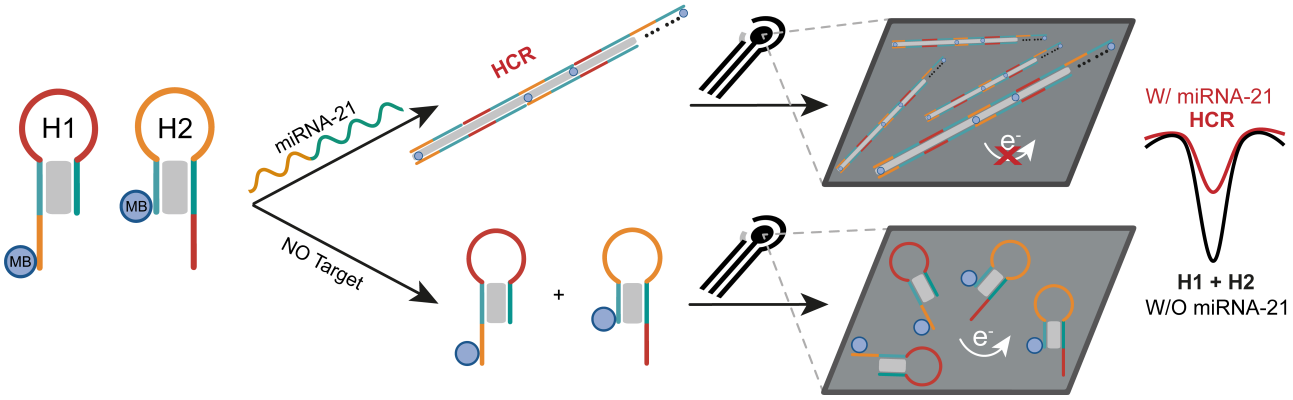

Scheme 1: Schematic representation illustrating the proposed HCR-based signal-off mechanism for the electrochemical detection of miRNA-21.

This signal-off mechanism offers high sensitivity, as even small amounts of miRNA-21 can cause a significant reduction in the electrochemical signal due to the amplification effect provided by HCR. The extent of the signal decrease is directly proportional to the concentration of the target miRNA-21, enabling accurate and highly sensitive quantification of miRNA.

The initial optimisation phase focused on selecting the optimal low-cost substrate for the screen-printed carbon electrodes, comparing polyester and chromatographic paper as shown in Figure 1A.

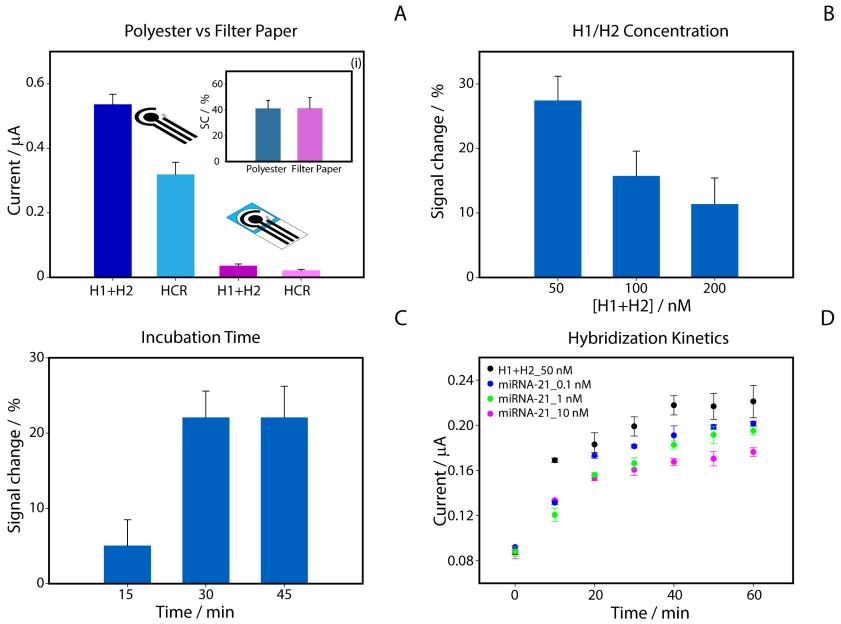

Figure 1: Optimization of the experimental parameters for miRNA-21 detection. A) Comparison of signal response on polyester (blue) and chromatographic paper (pink) substrates at 100 nM miRNA-21 concentration. Inset (i): Histogram showing signal change (%) in the presence of miRNA-21 on a polyester-based substrate (blue) and filter paper (pink). B) Optimization of H1+H2 concentrations (50, 100, and 200 nM); C) Evaluation

of incubation times (15, 30, and 45 minutes); D) Hybridization kinetics between H1 and H2 at 50 nM and varying miRNA-21 concentrations (0.1, 1, and 10 nM) over 60 minutes.

Despite a similar relative signal change % was observed when using a concentration of 100 nM miRNA-21, the polyester substrate was selected for its robustness and ability to generate a higher absolute current signal from the presence of MB.

In the context of HCR for miRNA-21 detection, the concentration of the two hairpin probes, H1 and H2, plays a crucial role in determining the resulting electrochemical signal. In order to maximize the signal change %, we tested different concentrations of H1+H2 at 50, 100 and 200 nM, keeping the concentration of miRNA-21 constant at 100 nM (Figure 1B). Consequently, another key aspect was the optimisation of the incubation time required for the HCR process. We first incubated H1+H2 at a concentration of 50 nM, both in the absence and presence of 100 nM miRNA-21, allowing the reaction to proceed for 15, 30, and 45 minutes, as shown in Figure 1C. Next, we evaluated the signal decrease rates of the H1+H2 solutions in the presence of the target miRNA-21 compared to the signal obtained with H1+H2 alone. The results showed that a reaction time of 30 minutes led to a 22% signal decrease, compared to only 5% decrease with 15-minute incubation. No significant difference was observed between 30 and 45 minutes. Therefore, we selected 30 minutes as the optimal incubation time for our analysis. Next, we studied the concentration dependence of the hybridisation kinetics, testing H1 and H2 at a concentration of 50 nM either alone or in the presence of miRNA-21 at concentrations of 0.1, 1 and 10 nM.. As shown in Figure 1D, a 30-minute incubation was sufficient to achieve both sensitivity and repeatability, as extending the time beyond 30 minutes did not significantly improve detection of different concentrations.

Analytical characterization in standard and human serum

After reviewing all key experimental features, we evaluated the analytical performance of the printed platform for HCR-based miRNA-21 detection. Initially, we conducted an evaluation in buffer solution by examining increasing concentrations of the target from 0.01 to 500 nM, as illustrated in Figure 2.

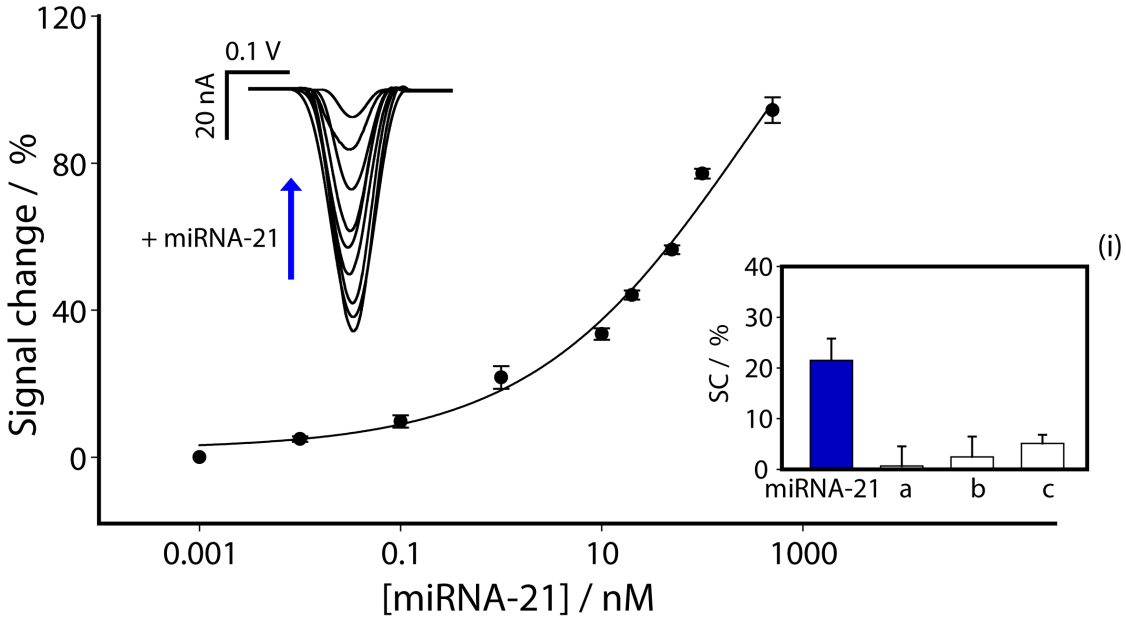

Figure 2: Calibration curve and SWV curves obtained in buffer solution by testing different concentrations of miRNA-21 target from 0.01 to 500 nM. Selectivity studies are reported in the inset (i) comparing the signal intensities obtained in the presence of not-complementary miRNAs. All the experiments have been carried out

in triplicate. SWV parameters: t eq=5 s, E start = 0.0 V, E end = −0.5 V, E step = 0.001 V, Amplitude = 0.01 V, Frequency = 50.0 Hz.

Optimised settings were applied for all experiments, revealing a semi-logarithmic sigmoidal relationship between signal change and target concentration (expressed on a logarithmic scale). It is important to highlight that the percentage signal change shown in the graphs reflects a reduction in the signal, as the system operates in a signal-off mode. The correlations were satisfactory, with a coefficient of determination R^2 of 0.993. Furthermore, the limit of detection (LOD) was calculated as the concentration corresponding to a 10% change in signal, approximately at 100 pM. The repeatability was good, with a coefficient of variation of 2% (calculated on five replicates at a target concentration of 50 nM). The results are highly promising, suggesting that the proposed HCR-based miRNA-21 detection platform offers significant potential for clinical application, particularly in terms of ease of use, short production time, high sensitivity and low cost. The platform's selectivity was also evaluated using four model interferents (miRNA-218, miRNA-29c-5p, miRNA-652-5p), each at a concentration of 0.1 nM. As shown in the inset of Figure 2, only minimal interference of up to 6 % was observed, confirming the specificity of the method in detecting miRNA-21, even in the presence of other miRNA species at similar concentrations.

After examining the platform's performance in model conditions, we extended our study to a complex biological matrix such as human serum. During the first tests with undiluted serum, we observed a significant matrix effect, which compromised effective reading of the electrochemical signal. This prompted us to conduct a thorough evaluation of the matrix effect, as illustrated in Figure 3A.

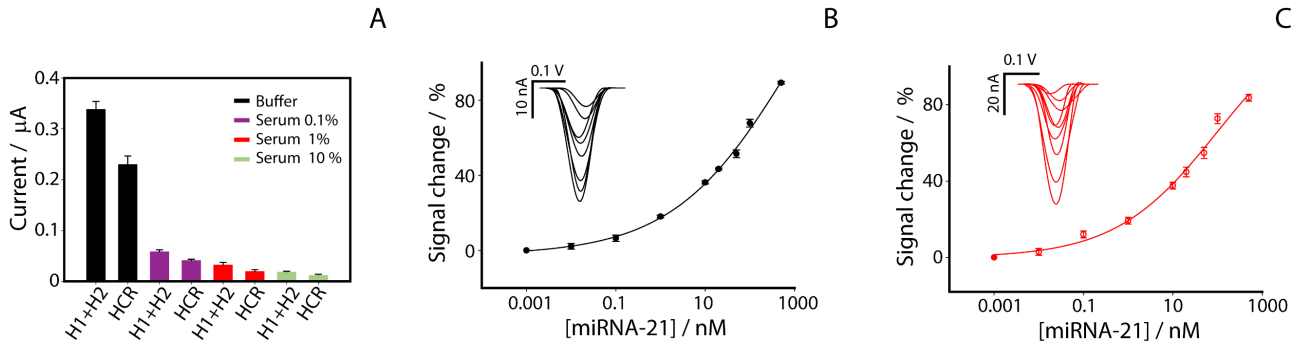

Figure 3: Characterisation of electrochemical sensor performance for miRNA-21 detection in buffer and human serum. A) Study of the matrix effect in the presence of 50 nM miRNA-21 in buffer (red) and human serum diluted to 0.1% (purple), 1% (orange) and 10% (green), before and after introduction of the miRNA-21 target. All bars were obtained as an average of three replicates; Calibration and SWV curves obtained in: B) Phosphate buffer using a H1/H2 concentration of 100 nM; C) 1% diluted serum using a H1/H2 concentration of 100 nM. All experiments were performed in triplicate and the experimental conditions are as shown in the caption of Figure 2.

To address this challenge, we decided to explore modifying the optimised concentration in buffer, and we tested the sensor using a H1 and H2 concentration of 100 nM together with a miRNA-21 concentration of 50 nM, in the presence of different serum dilutions (10%, 1%, 0.1%). The increase in H1 and H2 concentrations was thought to facilitate the detection of the electrochemical signal, counterbalancing the suppression effect observed in serum. As the graph in Figure 3 shows, even in the absence of the target, the absolute current value with only H1+H2 is significantly lower than that observed in buffer. However, the relative signal decrease percentages in the presence of miRNA-21 for all serum dilutions tested were similar to those achieved in buffer, being around 35%. These results indicate that, despite a significant matrix effect caused by human serum on the measurable currents, the sensor retains a good ability to discriminate and detect miRNA-21, exhibiting a consistent signal-off effect even under complex biological matrix conditions. This result is of

crucial importance for the potential deployment of the platform in clinical settings, where the ability to function effectively in the presence of biological matrices such as human serum is essential.

Next, we explored the performance of the sensor by testing it at different concentrations of miRNA-21, varying the concentrations of DNA hairpins H1 and H2 at 50 and 100 nM, and evaluating the performance in both phosphate buffer and serum diluted to 0.1% and 1%. As previously described, the calibration curve obtained in buffer using H1+H2 at a concentration of 50 nM demonstrated the ability to detect miRNA-21 up to 100 pM. In contrast, Figure 3B shows the calibration curve obtained in buffer with H1+H2 at a concentration of 100 nM. Under these conditions, the correlation yielded an R^2 value of 0.998, with a LOD set at 160 pM and a repeatability of 4%, calculated at a target concentration of 50 nM. To mitigate the matrix effect caused by serum, Figures 3C presents the calibration curve obtained in 1% serum, using H1+H2 at a concentration of 100 nM, with miRNA-21 concentrations ranging from 0.01 to 500 nM. The correlation was satisfactory, with determination coefficient of $R^2 = 0.993$, and a low limit of detection of 90 pM. Repeatability, calculated from five replicates at a target concentration of 50 nM, resulted to be ca. 5%.

Conclusions

In conclusion, this study developed and evaluated a highly sensitive platform for miRNA-21 detection, utilizing an electrochemical biosensor integrated with the hybridization chain reaction (HCR) on a polyester electrode. By eliminating the need for complex surface modifications, the platform significantly simplified the fabrication process, enhancing reproducibility and reducing production costs. The system demonstrated excellent sensitivity, with a detection limit in the picomolar range, and strong specificity, as evidenced by minimal interference from other closely related miRNAs. Moreover, the platform's robustness was validated in complex biological matrices, such as human serum, further highlighting its potential for clinical applications in disease diagnosis and monitoring. The results indicate that this biosensing approach is well-suited for point-of-care (PoC) diagnostics, offering a reliable, cost-effective tool for real-time miRNA analysis. Overall, this work not only advances electrochemical biosensor technology for miRNA detection but also paves the way for its practical use in clinical settings. It holds promise for enabling more precise and personalized disease management based on miRNA profiling, ultimately contributing to improved diagnostic and therapeutic strategies.

Acknowledgments

S.C. acknowledges funding from AIRC under the MFAG 2022 (ID 27586) project. This research was granted by University of Parma through the action Bando di Ateneo 2022 per la ricerca cofunded by MUR - Italian Ministry of Universities and Research−D.M. 737/2021- PNR-PNRR-NextGenerationEU. This work has benefited from the equipment and framework of the COMP-HUB and COMP-R Initiatives, funded by the “Departments of Excellence” program of the Italian Ministry for University and Research (MIUR, 2018-2022 and MUR,2023-2027).

(1) Yu, Z.; Zheng, Y.; Cai, H.; Li, S.; Liu, G.; Kou, W.; Yang, C.; Cao, S.; Chen, L.; Liu, X.; Wan, Z.; Zhang, N.; Li, X.; Cui, G.; Chang, Y.; Huang, Y.; Lv, H.; Feng, T. Molecular Beacon–Based Detection of Circulating microRNA-Containing Extracellular Vesicle as an α-Synucleinopathy Biomarker. *Science Advances* **2024**, *10* (20), eadl6442. https://doi.org/10.1126/sciadv.adl6442.

(2) Farazi, T. A.; Hoell, J. I.; Morozov, P.; Tuschl, T. MicroRNAs in Human Cancer. In *MicroRNA Cancer Regulation: Advanced Concepts, Bioinformatics and Systems Biology Tools*; Schmitz, U., Wolkenhauer, O., Vera, J., Eds.; Springer Netherlands: Dordrecht, 2013; pp 1–20. https://doi.org/10.1007/978-94-007-5590-1_1.

(3) Dong, H.; Lei, J.; Ding, L.; Wen, Y.; Ju, H.; Zhang, X. MicroRNA: Function, Detection, and Bioanalysis. *Chem. Rev.* **2013**, *113* (8), 6207–6233. https://doi.org/10.1021/cr300362f.
(4) Kulasingam, V.; Diamandis, E. P. Strategies for Discovering Novel Cancer Biomarkers through Utilization of Emerging Technologies. *Nat Rev Clin Oncol* **2008**, *5* (10), 588–599. https://doi.org/10.1038/ncponc1187.
(5) *Colocalization of protein and microRNA markers reveals unique extracellular vesicle subpopulations for early cancer detection | Science Advances*. https://www.science.org/doi/full/10.1126/sciadv.adh8689 (accessed 2024-06-26).
(6) Feng, Y.-H.; Tsao, C.-J. Emerging Role of microRNA-21 in Cancer (Review). *Biomedical Reports* **2016**, *5* (4), 395–402. https://doi.org/10.3892/br.2016.747.
(7) He, L.; Hannon, G. J. MicroRNAs: Small RNAs with a Big Role in Gene Regulation. *Nat Rev Genet* **2004**, *5* (7), 522–531. https://doi.org/10.1038/nrg1379.
(8) Bartel, D. P. MicroRNAs: Target Recognition and Regulatory Functions. *Cell* **2009**, *136* (2), 215–233. https://doi.org/10.1016/j.cell.2009.01.002.
(9) M. Zuidema, J.; Bertucci, A.; Kang, J.; J. Sailor, M.; Ricci, F. Hybrid Polymer/Porous Silicon Nanofibers for Loading and Sustained Release of Synthetic DNA-Based Responsive Devices. *Nanoscale* **2020**, *12* (4), 2333–2339. https://doi.org/10.1039/C9NR08474F.
(10) Bertucci, A.; Kim, K.-H.; Kang, J.; Zuidema, J. M.; Lee, S. H.; Kwon, E. J.; Kim, D.; Howell, S. B.; Ricci, F.; Ruoslahti, E.; Jang, H.-J.; Sailor, M. J. Tumor-Targeting, MicroRNA-Silencing Porous Silicon Nanoparticles for Ovarian Cancer Therapy. *ACS Appl. Mater. Interfaces* **2019**, *11* (27), 23926–23937. https://doi.org/10.1021/acsami.9b07980.
(11) Várallyay, É.; Burgyán, J.; Havelda, Z. MicroRNA Detection by Northern Blotting Using Locked Nucleic Acid Probes. *Nat Protoc* **2008**, *3* (2), 190–196. https://doi.org/10.1038/nprot.2007.528.
(12) Schmittgen, T. D.; Lee, E. J.; Jiang, J.; Sarkar, A.; Yang, L.; Elton, T. S.; Chen, C. Real-Time PCR Quantification of Precursor and Mature microRNA. *Methods* **2008**, *44* (1), 31–38. https://doi.org/10.1016/j.ymeth.2007.09.006.
(13) Thomson, J. M.; Parker, J.; Perou, C. M.; Hammond, S. M. A Custom Microarray Platform for Analysis of microRNA Gene Expression. *Nat Methods* **2004**, *1* (1), 47–53. https://doi.org/10.1038/nmeth704.
(14) Shen, Y.; Tian, F.; Chen, Z.; Li, R.; Ge, Q.; Lu, Z. Amplification-Based Method for microRNA Detection. *Biosensors and Bioelectronics* **2015**, *71*, 322–331. https://doi.org/10.1016/j.bios.2015.04.057.
(15) Ouyang, T.; Liu, Z.; Han, Z.; Ge, Q. MicroRNA Detection Specificity: Recent Advances and Future Perspective. *Anal. Chem.* **2019**, *91* (5), 3179–3186. https://doi.org/10.1021/acs.analchem.8b05909.
(16) Miao, J.; Wang, J.; Guo, J.; Gao, H.; Han, K.; Jiang, C.; Miao, P. A Plasmonic Colorimetric Strategy for Visual miRNA Detection Based on Hybridization Chain Reaction. *Sci Rep* **2016**, *6* (1), 32219. https://doi.org/10.1038/srep32219.
(17) Dehnoei, M.; Ahmadi-Sangachin, E.; Hosseini, M. Colorimetric and Fluorescent Dual-Biosensor Based on Zirconium and Preasodium Metal-Organic Framework (Zr/Pr MOF) for miRNA-191 Detection. *Heliyon* **2024**, *10* (6), e27757. https://doi.org/10.1016/j.heliyon.2024.e27757.
(18) Yu, Y.; Chen, Z.; Shi, L.; Yang, F.; Pan, J.; Zhang, B.; Sun, D. Ultrasensitive Electrochemical Detection of MicroRNA Based on an Arched Probe Mediated Isothermal Exponential Amplification. *Anal. Chem.* **2014**, *86* (16), 8200–8205. https://doi.org/10.1021/ac501505a.
(19) Zhang, L.; Su, W.; Liu, S.; Huang, C.; Ghalandari, B.; Divsalar, A.; Ding, X. Recent Progresses in Electrochemical DNA Biosensors for MicroRNA Detection. *Phenomics* **2022**, *2* (1), 18–32. https://doi.org/10.1007/s43657-021-00032-z.
(20) Jolly, P.; Batistuti, M. R.; Miodek, A.; Zhurauski, P.; Mulato, M.; Lindsay, M. A.; Estrela, P. Highly Sensitive Dual Mode Electrochemical Platform for microRNA Detection. *Sci Rep* **2016**, *6* (1), 36719. https://doi.org/10.1038/srep36719.
(21) Singh, S.; Miglione, A.; Raucci, A.; Numan, A.; Cinti, S. Towards Sense and Sensitivity-Based Electrochemical Biosensors for Liquid Biopsy-Based Breast Cancer Detection. *TrAC Trends in Analytical Chemistry* **2023**, *163*, 117050. https://doi.org/10.1016/j.trac.2023.117050.
(22) Kjällman, T. H. M.; Peng, H.; Soeller, C.; Travas-Sejdic, J. Effect of Probe Density and Hybridization Temperature on the Response of an Electrochemical Hairpin-DNA Sensor. *Anal. Chem.* **2008**, *80* (24), 9460–9466. https://doi.org/10.1021/ac801567d.
(23) Lubin, A. A.; Vander Stoep Hunt, B.; White, R. J.; Plaxco, K. W. Effects of Probe Length, Probe Geometry, and Redox-Tag Placement on the Performance of the Electrochemical E-DNA Sensor. *Anal. Chem.* **2009**, *81* (6), 2150–2158. https://doi.org/10.1021/ac802317k.

(24) Fortunati, S.; Vasini, I.; Giannetto, M.; Mattarozzi, M.; Porchetta, A.; Bertucci, A.; Careri, M. Controlling Dynamic DNA Reactions at the Surface of Single-Walled Carbon Nanotube Electrodes to Design Hybridization Platforms with a Specific Amperometric Readout. *Anal. Chem.* **2022**, *94* (12), 5075–5083. https://doi.org/10.1021/acs.analchem.1c05294.
(25) Li, B.; Jiang, Y.; Chen, X.; Ellington, A. D. Probing Spatial Organization of DNA Strands Using Enzyme-Free Hairpin Assembly Circuits. *J. Am. Chem. Soc.* **2012**, *134* (34), 13918–13921. https://doi.org/10.1021/ja300984b.
(26) Liu, H.; Li, L.; Duan, L.; Wang, X.; Xie, Y.; Tong, L.; Wang, Q.; Tang, B. High Specific and Ultrasensitive Isothermal Detection of MicroRNA by Padlock Probe-Based Exponential Rolling Circle Amplification. *Anal. Chem.* **2013**, *85* (16), 7941–7947. https://doi.org/10.1021/ac401715k.
(27) Liu, Y.-Q.; Zhang, M.; Yin, B.-C.; Ye, B.-C. Attomolar Ultrasensitive MicroRNA Detection by DNA-Scaffolded Silver-Nanocluster Probe Based on Isothermal Amplification. *Anal. Chem.* **2012**, *84* (12), 5165–5169. https://doi.org/10.1021/ac300483f.
(28) *Design and Analysis of Localized DNA Hybridization Chain Reactions - Bui - 2017 - Small - Wiley Online Library*. https://onlinelibrary.wiley.com/doi/full/10.1002/smll.201602983 (accessed 2024-06-25).
(29) Dirks, R. M.; Pierce, N. A. Triggered Amplification by Hybridization Chain Reaction. *Proceedings of the National Academy of Sciences* **2004**, *101* (43), 15275–15278. https://doi.org/10.1073/pnas.0407024101.
(30) Wu, J.; Lv, J.; Zheng, X.; Wu, Z.-S. Hybridization Chain Reaction and Its Applications in Biosensing. *Talanta* **2021**, *234*, 122637. https://doi.org/10.1016/j.talanta.2021.122637.
(31) Bi, S.; Yue, S.; Zhang, S. Hybridization Chain Reaction: A Versatile Molecular Tool for Biosensing, Bioimaging, and Biomedicine. *Chemical Society Reviews* **2017**, *46* (14), 4281–4298. https://doi.org/10.1039/C7CS00055C.
(32) Evanko, D. Hybridization Chain Reaction. *Nat Methods* **2004**, *1* (3), 186–186. https://doi.org/10.1038/nmeth1204-186a.
(33) Zhang, C.; Chen, J.; Sun, R.; Huang, Z.; Luo, Z.; Zhou, C.; Wu, M.; Duan, Y.; Li, Y. The Recent Development of Hybridization Chain Reaction Strategies in Biosensors. *ACS Sens.* **2020**, *5* (10), 2977–3000. https://doi.org/10.1021/acssensors.0c01453.
(34) Xia, N.; Cheng, J.; Tian, L.; Zhang, S.; Wang, Y.; Li, G. Hybridization Chain Reaction-Based Electrochemical Biosensors by Integrating the Advantages of Homogeneous Reaction and Heterogeneous Detection. *Biosensors* **2023**, *13* (5), 543. https://doi.org/10.3390/bios13050543.
(35) Zhang, Q. Application of Hybridization Chain Reaction (HCR) in Electrochemical Analysis. *International Journal of Electrochemical Science* **2022**, *17* (2), 220227. https://doi.org/10.20964/2022.02.14.
(36) Ge, Z.; Lin, M.; Wang, P.; Pei, H.; Yan, J.; Shi, J.; Huang, Q.; He, D.; Fan, C.; Zuo, X. Hybridization Chain Reaction Amplification of MicroRNA Detection with a Tetrahedral DNA Nanostructure-Based Electrochemical Biosensor. *Anal. Chem.* **2014**, *86* (4), 2124–2130. https://doi.org/10.1021/ac4037262.
(37) *MicroRNA detection based on analyte triggered nanoparticle localization on a tetrahedral DNA modified electrode followed by hybridization chain reaction dual amplification - Chemical Communications (RSC Publishing)*. https://pubs.rsc.org/en/content/articlelanding/2015/cc/c5cc05499k/unauth (accessed 2024-06-25).
(38) Zhai, Q.; He, Y.; Li, X.; Guo, J.; Li, S.; Yi, G. A Simple and Ultrasensitive Electrochemical Biosensor for Detection of microRNA Based on Hybridization Chain Reaction Amplification. *Journal of Electroanalytical Chemistry* **2015**, *758*, 20–25. https://doi.org/10.1016/j.jelechem.2015.10.010.
(39) *Multiple Amplified Electrochemical Detection of MicroRNA-21 Using Hierarchical Flower-like Gold Nanostructures Combined with Gold-enriched Hybridization Chain Reaction - Zhu - 2018 - Electroanalysis - Wiley Online Library*. https://analyticalsciencejournals.onlinelibrary.wiley.com/doi/full/10.1002/elan.201700696?casa_token=yu2SkkuhjkIAAAAA%3AT0EOPdgC5Ay2CSOlqnnMHjyR2JzA5pnW-22l3MvSPqgCxA8oeJlPJ4fVEvHTw_qDd9ywsp7rb-Z61QZO (accessed 2024-06-25).
(40) Liu, H.; Bei, X.; Xia, Q.; Fu, Y.; Zhang, S.; Liu, M.; Fan, K.; Zhang, M.; Yang, Y. Enzyme-Free Electrochemical Detection of microRNA-21 Using Immobilized Hairpin Probes and a Target-Triggered Hybridization Chain Reaction Amplification Strategy. *Microchim Acta* **2016**, *183* (1), 297–304. https://doi.org/10.1007/s00604-015-1636-z.

(41) Hou, T.; Li, W.; Liu, X.; Li, F. Label-Free and Enzyme-Free Homogeneous Electrochemical Biosensing Strategy Based on Hybridization Chain Reaction: A Facile, Sensitive, and Highly Specific MicroRNA Assay. *Anal. Chem.* **2015**, *87* (22), 11368–11374. https://doi.org/10.1021/acs.analchem.5b02790.
(42) Cinti, S.; Moscone, D.; Arduini, F. Preparation of Paper-Based Devices for Reagentless Electrochemical (Bio)Sensor Strips. *Nat Protoc* **2019**, *14* (8), 2437–2451. https://doi.org/10.1038/s41596-019-0186-y.
(43) Raucci, A.; Cimmino, W.; Grosso, S. P.; Normanno, N.; Giordano, A.; Cinti, S. Paper-Based Screen-Printed Electrode to Detect miRNA-652 Associated to Triple-Negative Breast Cancer. *Electrochimica Acta* **2024**, *487*, 144205. https://doi.org/10.1016/j.electacta.2024.144205.